GMR
The Original

FORMULATION AND QBD-BASED OPTIMIZATION OF CHITOSAN-COATED NANOSTRUCTURED LIPID CARRIERS FOR ENHANCED DRUG DELIVERY OF AZILSARTAN MEDOXOMIL

Jeyaprabha Ponnusamy[1]*, Saravanan Gopal[2]

[1,2] Faculty of Pharmacy, Karpagam Academy of Higher Education, Coimbatore-641021, Tamil Nadu, India.
*Corresponding Author: Jeyaprabha Ponnusamy, E-mail: jayaprava@gmail.com

ABSTRACT

Objective: Azilsartan medoxomil (AZM) is a Class II antihypertensive drug with poor aqueous solubility that limit its dissolution and oral performance. The aim of present investigation was to improve its dissolution properties by formulating chitosan-coated AZM NLCs (CH-NLCs) and optimizing using QbD approach.

Methods: Oleic acid, Compritol® 888 ATO, Kolliphor® RH 40, Chitosan as a liquid lipid, solid lipid, coating polymer and surfactant respectively. Chitosan coated AZM- NLCs were prepared by hot homogenization-ultrasonication method and optimized using BBD. Particle size, entrapment efficiency, zeta potential, DSC, FTIR, SEM and X-RD and release studies were evaluated.

Results: Optimized CH-NLCs displayed particle size (172.25 ± 5.09 nm), entrapment efficiency (85.04 ± 2.61%), and zeta potential (+36.2 ± 1.2 mV). Solid-state analysis indicated reduced crystallinity and amorphous dispersion of AZM within the lipid–polymer matrix. The *in vitro* drug release (~92% over 24 h) showed diffusion-controlled release kinetics.

Conclusion: The results of chitosan coated NLCs showed better drug loading and controlled release behaviour. The study suggests the potential of CH-NLCs for improved oral delivery.

KEYWORDS: Azilsartan medoxomil, Chitosan-coated nanostructured lipid carriers, Quality by Design (QbD), Entrapment efficiency, Amorphous drug dispersion, Oral drug delivery.

GRAPHICAL ABSTRACT

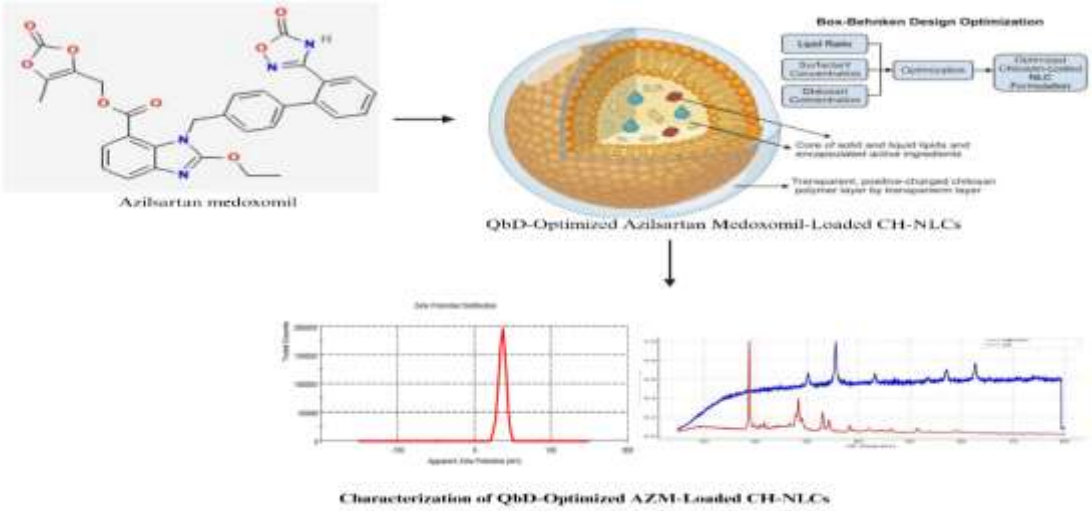

INTRODUCTION

Azilsartan medoxomil (AZM) is a popular selective angiotensin II type 1 (AT 1) receptor blocker used to treat hypertension. Although AZM has a powerful antihypertensive effect, it is a BCS Class II medication, which is highly permeable but not very soluble in aqueous extracts [1]. Its poor solubility in the gastrointestinal fluids may limit oral bioavailability and add to the fluctuation in therapeutic performance. Thus, formulation techniques that would promote dissolution behaviour and stability are of significant interest [2].

Drug delivery systems based on lipids have become promising platform to enhance the performances of drugs that are poorly soluble [3]. Among them, nanostructured lipid carriers (NLCs) which consist of a blend between solid and liquid

lipids offer a partially disordered network that improves drug accommodation and decreases the likelihood of drug release during storage [4,5]. Their small size (nanoscale) means that they can be better dispersed and have a controlled release behaviour, and this makes them good candidates when it comes to the oral delivery of lipophilic compounds like AZM [6].

Surface coating of lipid nanoparticles was also undertaken to further streamline interfacial characteristics and release behaviours. Chitosan is bioadhesive cationic polysaccharide, used as a coating polymer since it can adsorb onto negatively charged lipid surfaces via electrostatic interactions [7]. This type of modification can also change surface charge, promote dispersion stability and create an additional diffusional barrier that can regulate the release of drugs [8].

Despite the reported lipid-based formulations of AZM, systematic optimization of chitosan-coated NLCs based on a Quality by Design (QbD) model is not extensively described [9]. QbD is a systematic format of pharmaceutical development in which essential material qualities and process parameters are determined and managed that impact important quality qualities [10]. In this context, response surface techniques like BBD can be used to effectively analyze the variables of formulations and their interrelations [11].

The current paper had the objective of designing and optimizing nanostructured lipid carriers of AZM by coating them with chitosan in a QbD-based strategy [12]. The effect of lipid, surfactant & chitosan on the size of particles, entrapment efficiency, and drug release was investigated in a systematic manner so as to achieve a strong and repeatable formulation with the desired release property [13].

MATERIALS AND METHODS

Materials

Azilsartan medoxomil (AZM), sourced from a pharmaceutical manufacturer (India). Compritol® 888 ATO (glyceryl behenate) and oleic acid served as solid and liquid lipids, respectively. Kolliphor® RH 40 was used as surfactant [14]. Chitosan (85% deacetylation, ~150 kDa) was the coating polymer [15]. All other reagents were analytical grade from standard suppliers. Distilled water was utilized throughout the study [16].

Preparation of AZM-Incorporated NLCs

AZM (50 mg) was incorporated into a lipid phase (Compritol® 888 ATO 150 mg + oleic acid 50 mg, 75:25 w/w ratio) heated to 75–80 °C to get a clear melt [17]. Kolliphor® RH 40 (100 mg) in distilled water at the same temperature (20 mL) to melted lipid phase. A coarse emulsion was produced by high-speed homogenization (15,000 rpm, 10 min) [18]. Probe ultrasonication (8 min, 60% amplitude, pulsing) generated a nanoemulsion that was cooled to room temperature to solidify lipids and generate nanostructured lipid carriers [19]. The dispersion was kept at 4 °C till characterisation [20].

Preparation of Chitosan-Coated NLCs [21,22,23]

Chitosan (1.0% w/v) dissolved in 0.5% acetic acid was pH-adjusted to 4.8 ± 0.2 with 0.1 N NaOH to protonate amino groups. The NLC dispersion was mixed with chitosan solution (1:4 ratio) at 600 rpm for 4 h at room temperature for electrostatic adsorption onto the NLC surface. The CH-NLC dispersion was equilibrated for 1 h and stored at 4 °C.

Experimental Design

BBD was used to fix formulation factors: solid/liquid lipid content (Compritol® 888 ATO and oleic acid), surfactant concentration (Kolliphor® RH 40), and chitosan concentration. Each factor was analyzed at 3 levels (-1, 0, +1) to assess impact on dependent variables—particle size and entrapment efficiency—to enhance stability, drug loading, and sustained release characteristics [24- 26].

Table 1. BBD Matrix for Optimization of AZM -Chitosan-Coated Nanostructured Lipid Carriers (CH-NLCs)

Factor	Independent Variable	Level -1	Level 0	Level +1
X_1	Lipid concentration (%)	50	75	100
X_2	Surfactant concentration (%)	2.5	5.0	7.5
X_3	Chitosan concentration (%)	0.5	1.0	1.5

Table 2. Dependent Variables (Responses) and Optimization Goals

Response	Measured Parameter	Desired outcome
Y_1	Particle Size (nm)	Decrease
Y_2	Entrapment Efficiency (%)	Increase
Y_3	Cumulative Drug Release (%)	Optimize for sustained release

Characterization Studies

Once formulations were prepared according to the BBD matrix, each batch was subjected to the following characterization:

Particle Size & Polydispersity Index (PDI):
DLS was used to measure particle size and PDI. To prevent several scattering effects, the samples were diluted 1:20 (v/v) using filtered distilled water and the samples were analysed thrice (n = 3) [27].

Zeta Potential:
The value of zeta potential was obtained at the same instrument by electrophoretic light scattering. Samples were diluted 1:20 (v/v) with distilled water, the observations were conducted at 25 ± 0.5 °C, and each sample was studied thrice (n = 3) [28].

SEM:
Before morphological analysis, NLC and CH-NLC dispersions were lyophilized prior to imaging. A 5% w/v mannitol solution was used as a cryoprotectant. Surface morphology was studied using Scanning Electron Microscope (JEOL JSM-7610F, Japan) at an accelerating voltage of 10 kV [29].

FTIR Analysis:
FTIR spectra of AZM, lipids, physical mixture, and CH-NLC were captured using an FTIR spectrophotometer (PerkinElmer Spectrum Two, USA) in ATR mode. Samples were scanned over a range of 4000–400 cm^{-1} at a resolution of 4 cm^{-1}, with 32 scans per sample [30].

XRD:
XRD analysis was conducted using an X-ray diffractometer. Samples were scanned over a 2θ range of 5°–50° at a scanning rate of 2°/min with a step size of 0.02°. Diffractograms of AZM, lipid excipients, physical mixture, and CH-NLC were recorded for comparison [31].

DSC:
About 5 mg of AZM, lipid mixture, physical mixture, and CH-NLC were loaded in sealed aluminium pans. Thermal analysis was performed using a DSC instrument (TA Instruments Q2000, USA). [32].

EE %:
EE% was quantified by separating the unencapsulated drug from the nanoparticle dispersion using ultracentrifugation. Briefly, 2 mL of AZM-NLC dispersion was centrifuged, supernatant containing unentrapped drug was carefully collected and the amount of free AZM was quantified at 249nm.

$$EE\% = \frac{(W_{total} - W_{free})}{W_{total}} \times 100$$

where W_{total} is the total amount of drug added and W_{free} is the amount of drug detected in the supernatant. All observations were taken in three replicates (n = 3), results were expressed as mean ± standard deviation.

In Vitro Drug Release Study
Drug release of AZM from NLC and CH-NLC formulations were studied using the dialysis bag diffusion technique. To summarize, 2 mL of nanoformulation (equivalent to 5 mg AZM) was loaded into pre-soaked cellulose membranes (MWCO 12,000–14,000 Da) and immersed in 100 mL phosphate buffer (pH 6.8) containing 0.5% w/v Tween 80. The study was performed using a USP Type II apparatus at 37 ± 0.5 °C and 100 rpm [33,34].
At predetermined intervals (0.5–24 h), 2 mL were removed and replenished with fresh medium. (<10% saturation solubility). Samples were studied at 249 nm using a UV–Visible spectrophotometer. Data were presented as cumulative percentage drug release (mean ± SD, n = 3), with free AZM solution and uncoated NLCs as controls.

Release Kinetics
Release findings were fitted to zero-order, first-order, Higuchi, Korsmeyer–Peppas, and Hixson–Crowell models. The best-fit model was selected based on the highest R^2 value, while the release exponent (n) from the Korsmeyer–Peppas model indicated the release mechanism. Nonlinear regression was performed using Prism software.

Design of Experiments (DoE)
A 3-level, 3-factor BBD was utilized in the study. Lipid concentration (X_1), surfactant concentration (X_2) and chitosan concentration (X_3) were chosen as the independent variables. The dependent variables were particle size (Y1), entrapment efficiency (Y_2) and cumulative release of the drug (Y_3). Cumulative drug release (Y_3) was measured after 24 h because this time was deemed to be reflective of sustained drug release which was reported in Table 3.

Table 3. Experimental Runs and Measured Responses for BBD Optimization of CH-NLCs

Std	Run	Factor 1	Factor 2	Factor 3	Response 1	Response 2	Response 3
		A: Chitosan	B: Lipid Con.	C: Surfactant	Particle size	Entrapment efficiency	Drug release
		%	%	%	nm	%	%
14	1	1	75	5	152.91± 2.62	81.06 ± 1.60	92.02 ± 1.63
16	2	1	75	5	152.91± 2.62	81.06 ± 1.60	92.02 ± 1.63
1	3	0.5	50	5	229.04± 7.23	53.89 ± 1.42	87.91 ± 2.20
3	4	0.5	100	5	297.37± 8.22	74.69 ± 2.38	82.45 ± 2.84
17	5	1	75	5	152.91± 2.62	81.06 ± 1.60	92.02 ± 1.63
8	6	1.5	75	7.5	205.49± 5.27	44.33 ± 1.55	78.22 ± 2.35
5	7	0.5	75	2.5	185.57± 5.22	74.43 ± 1.11	89.23 ± 2.80
11	8	1	50	7.5	259.93± 4.22	71.05 ± 1.97	70.33 ± 2.34
6	9	1.5	75	2.5	185.75± 3.71	32.90 ± 2.54	52.23 ± 3.06
10	10	1	100	2.5	198.37± 7.92	63.44 ± 2.53	62.47 ± 2.56

4	11	1.5	100	5	174.75± 4.49	35.73 ± 2.13	84.24 ± 3.30
7	12	0.5	75	7.5	311.06± 5.24	43.67 ± 2.56	35.03 ± 4.07
2	13	1.5	50	5	188.01± 2.76	63.19 ± 2.69	80.34 ± 1.84
9	14	1	50	2.5	165.70± 4.31	74.52 ± 3.54	63.05 ± 3.25
15	15	1	75	5	152.91± 2.62	81.06 ± 1.60	92.02 ± 1.63
12	16	1	100	7.5	285.63± 4.80	65.05 ± 3.84	34.86 ± 4.33
13	17	1	75	5	152.91± 2.62	81.06 ±1.60	92.02 ± 1.63

Statistical Analysis and Model Evaluation

All studies were analysed thrice (n = 3) and expressed as mean ± SD. Studied using BBD with Design-Expert® software (Version 13.0, Stat-Ease Inc., USA).

ANOVA was used to evaluate the significance of the models, and adequacy was assessed based on F-value, p-value, R^2, adjusted R^2**, ** predicted R^2**, ** and lack-of-fit. A p-value < 0.05 was considered statistically significant. Regression equations were generated, and response surface plots were constructed to illustrate variable interactions.

Data were analyzed to compare uncoated and chitosan-coated formulations using one-way ANOVA with appropriate post hoc tests ($p < 0.05$).

RESULTS

Optimization via BBD

The Box–Behnken Design (BBD) established the significance of three formulation parameters chitosan concentration (A), lipid density (B), and surfactant concentration (C) for modulating CQAs such as particle size(Y_1) entrapment efficiency(Y_2) and drug release(Y_3). The fitted regression equation was statistically analysed and the quadratic model was found significant ($F = 9.58$; $p = 0.0035$), which suggested a good fit of the experimental data. The model demonstrated excellent correlation coefficients ($R^2 > 0.95$), and a non-significant lack-of-fit test indicated its predictive accuracy.

Results Regression analysis indicated significant impacts of chitosan and surfactant concentrations on the particle size and entrapment efficiency ($P < 0.05$). Higher concentrations of chitosan resulted in larger particles due to the creation of a polymeric layer around the lipid core, while increased surfactant concentration produced smaller particles because interfacial tension was reduced and emulsification improved. This indicates that varying lipid concentration has a moderate influence affecting drug entrapment and matrix integrity.

The optimized formulation derived using the desirability function approach achieved a balance among all three CQAs. The predicted values from the model were closely aligned with experimental results (Table 1), confirming the robustness of the optimization process.

$$Y=\beta0+\beta1X_1+\beta2X_2+\beta3X_3+\beta12X_1X_2+\beta13X_1X_3+\beta23X_2X_3+\beta11X_1^2+\beta22X_2^2+\beta33X_3^2$$

where Y represents the response variable, β denotes the regression coefficient, X_1, X_2, X_3 factors A, B, and C, respectively. Figures 1, 2 & 3 indicated that stirring speed was the key factor for all three parameters. Finding the optimal chitosan concentration was crucial to appropriately tuning particle size, entrapment efficiency, and drug release. Chitosan at moderate levels produced small, dispersed particles with both high drug loading and sustained release, while excessive amounts promoted increased size and aggregation. Justification of the optimization model for AZM-loaded chitosan-coated NLC formulation.

Three-dimensional (3D) response surface plots were constructed to illustrate the effect of each independent variable on each response. These are plots of curvature and interaction effects, essentially a visual representation of that optimization space. The particle size surface, for example, showed that larger particles were achieved with higher chitosan concentration and smaller particle sizes were reached at low starting surfactant level; a more uniform range of regularized intermediate-sized particles was formed with an intermediate surfactant level. The plot of entrapment efficiency presented maximum values that resulted from depleted polymer adsorption over compactness of the matrix. This is achieved at moderate lipid concentration and moderately high chitosan (CS) concentrations suggesting an optimal balance.

Table 4. Quadratic Model Fitting of Particle Size (Response Y_1)

Source	**Sum of Squares**	**Df**	**Mean Square**	**F-Value**	**p-value**
Model	36935.93	9	4103.99	9.58	0.0035
A-Chitosan	9870.13	1	9870.13	23.03	0.0020
B-Lipid Concentration	1800.00	1	1800.00	4.20	0.0796
C-Surfactant Concentration	13203.13	1	13203.13	30.81	0.0009
AB	1640.25	1	1640.25	3.83	0.0913
AC	3025.00	1	3025.00	7.06	0.0326

BC	0.2500	1	0.2500	0.0006	0.9814
A^2	1296.85	1	1296.85	3.03	0.1255
B^2	2912.38	1	2912.38	6.80	0.0351
C^2	2435.38	1	2435.38	5.68	0.0486
Residual	2999.95	7	428.56		
Lack of Fit	718.75	3	239.58	0.4201	0.7490
Pure Error	2281.20	4	570.30		
Cor Total	39935.88	16			

ANOVA results reported (Table 4) demonstrated the statistical significance of the (F = 9.58, p = 0.0035), and good fit (lack of fit p = 0.7490). The concentration of chitosan had the most significant (F = 23.03, p = 0.0020), followed by surfactant (F = 30.81, p = 0.0009) and lipid concentrations with moderate but non-significant effects (F = 4.20, p = 0.0796). Only the interaction of chitosan and surfactant was significant (F = 7.06, p = 0.0326) while interactions with other components were not significant. Lipid and surfactant quadratic effects ($p < 0.05$) were significant, reflecting non-linearity. In general, the determining factors for formulation performance were chitosan and surfactant concentrations while lipid concentration had a secondary effect.

Particle Size = $178.4-35.13A+15.00B+40.63C-20.25AB-27.50AC-0.25BC+17.55A^2+26.30B^2+24.05C^2$

The equation suggests that chitosan concentration is the most influential factor, significantly increasing particle size, while lipid and surfactant concentrations have relatively smaller effects. The interaction terms indicate complex relationships, particularly between chitosan and surfactant concentration, which significantly reduces particle size when increased together.

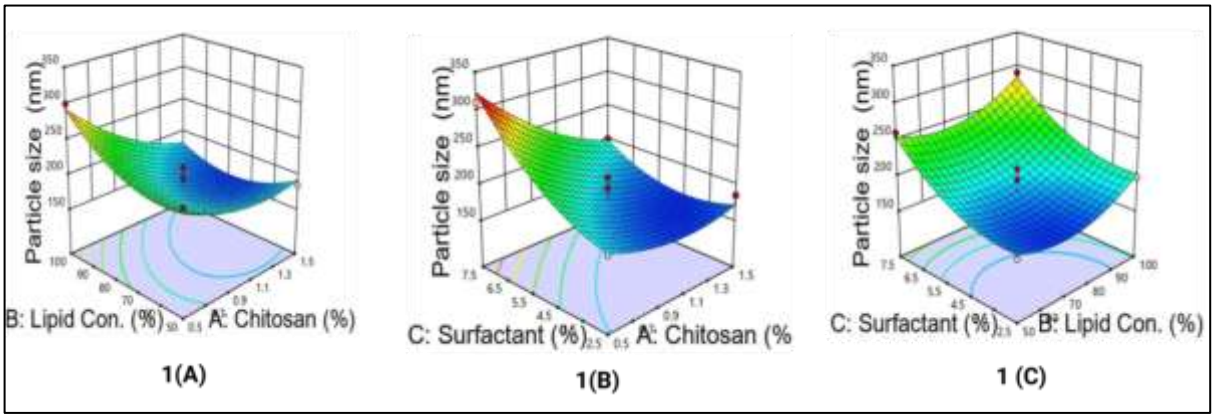

Fig.1: showing (A) Effect of chitosan and lipid concentration. (B) Effect of lipid and surfactant concentration. (C) Effect of chitosan and surfactant concentration on particle size.

Table 5. Quadratic Model Fitting of Entrapment Efficiency (Response Y_2)

Source	Sum of Squares	df	Mean Square	F-value	p-value	
Model	4727.30	9	525.26	39.77	< 0.0001	significant
A-Chitosan	651.24	1	651.24	49.31	0.0002	
B-Lipid Con.	60.61	1	60.61	4.59	0.0694	
C-Surfactant	71.52	1	71.52	5.42	0.0528	
AB	724.69	1	724.69	54.87	0.0001	
AC	433.89	1	433.89	32.85	0.0007	
BC	0.9409	1	0.9409	0.0712	0.7972	
A^2	2177.30	1	2177.30	164.85	< 0.0001	
B^2	9.22	1	9.22	0.6983	0.4310	
C^2	448.87	1	448.87	33.99	0.0006	
Residual	92.45	7	13.21			
Lack of Fit	87.44	3	29.15	23.28	0.0054	Not significant
Pure Error	5.01	4	1.25			
Cor Total	4819.75	16				

The ANOVA results (Table 5) show the quadratic model is highly significant ($p < 0.0001$) for predicting entrapment

efficiency. Chitosan concentration (p = 0.0002) had the greatest effect, while lipid (p = 0.0694) and surfactant (p = 0.0528) showed moderate influence. Significant interactions (AB, AC; p < 0.001) and quadratic effects of chitosan and surfactant (p < 0.001) indicate nonlinear relationships. Despite a significant lack of fit (p = 0.0054), chitosan remains the dominant factor governing entrapment efficiency.

Entrapment Efficiency = 81.48−9.02A−2.75B−2.99C−13.46AB+10.42AC+0.49BC−22.74A^2−1.48B^2−10.33C^2

The regression equation for Entrapment Efficiency indicates a nonlinear relationship between chitosan (A), lipid (B), and surfactant (C) concentrations. Chitosan has the most significant negative impact, reducing entrapment efficiency as its concentration increases. The interaction term AB (chitosan and lipid) negatively affects efficiency, whereas AC (chitosan and surfactant) has a positive effect.

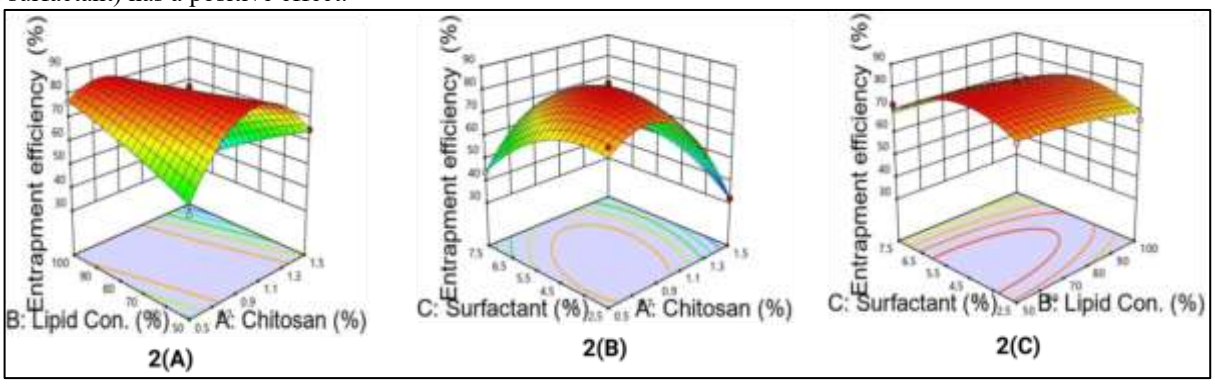

Fig.2: showing (A) Effect of chitosan and lipid concentration. (B) Effect of lipid and surfactant concentration. (C) Effect of chitosan and surfactant concentration on entrapment efficiency (EE%).

Table 6. Quadratic Model Fitting of Drug Release (Response Y_3)

Source	Sum of Squares	Df	Mean Square	F-value	p-value	Significance
Model	5452.92	9	605.88	17.56	0.0005	Significant
A – Chitosan	1.13	1	1.13	0.0326	0.8618	Not significant
B – Lipid Concentration	162.00	1	162.00	4.69	0.0669	Not significant
C – Surfactant	253.13	1	253.13	7.34	0.0303	Significant
AB	42.25	1	42.25	1.22	0.3051	Not significant
AC	1521.00	1	1521.00	44.08	0.0003	Significant
BC	272.25	1	272.25	7.89	0.0262	Significant
A^2	15.20	1	15.20	0.4405	0.5281	Not significant
B^2	144.09	1	144.09	4.18	0.0803	Not significant
C^2	2979.20	1	2979.20	86.34	< 0.0001	Significant
Residual	241.55	7	34.51	–	–	–
Lack of Fit	114.75	3	38.25	1.21	0.4147	Not significant
Pure Error	126.80	4	31.70	–	–	–
Cor Total	5694.47	16	–	–	–	–

The ANOVA results (Table 6) for the quadratic model of drug release, where the p-value indicates that the model is significant (p = 0.0005), suggesting its suitability to explain variation in drug release. The individual effects show that surfactant concentration (C) had a significant impact (p = 0.0303), while lipid concentration (B) showed a moderate effect (p = 0.0669). The effect of chitosan concentration (A) on drug release was not significant (p = 0.8618). The interaction effects reveal that drug release is significantly influenced by AC (chitosan and surfactant) as well as BC (lipid and surfactant), with the strongest effect observed for AC (p = 0.0003). Both C^2 and B^2 were included as quadratic terms, with C^2 being highly significant (p < 0.0001), indicating strong nonlinear effects, whereas B^2 was not significant (p = 0.0803). The model showed a good fit, with a non-significant lack-of-fit (p = 0.4147). These findings highlight the importance of surfactant concentration and its interactions in drug release, while chitosan showed negligible impact.

Drug release = 89.20−0.38A−4.50B−5.63C+3.25AB+19.50AC−8.25BC+1.90A^2−5.85B^2−26.60C^2

The model for drug release follows a quadratic relation, showing strong correlation between formulation variables. The concentration of surfactant had the greatest influence (strong quadratic effect, C^2, p < 0.0001), suggesting that very high or low values hinder drug release. Additionally, the interaction of chitosan and surfactant is also significant (p = 0.0003),

indicating that these two factors have a synergistic influence on the response. Lipid showed a moderate contribution (B^2 term included due to quadratic effect), while chitosan contributed minimally.
The model was significant ($p = 0.0005$), and the lack of fit was non-significant ($p = 0.4147$), indicating good prediction of drug release patterns by the Box–Behnken design.

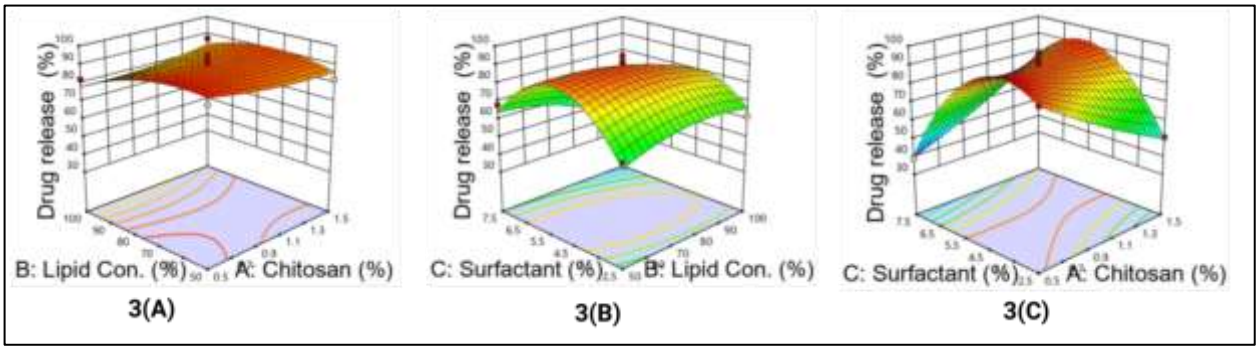

Fig. 3a, 3b, and 3c: The 3D response surface plots illustrate on drug release. (A) Effect of chitosan and lipid concentration. (B) Effect of lipid and surfactant concentration. (C) Effect of chitosan and surfactant concentration.

Particle Size and PDI
The average particle size and PDI were obtained using dynamic light scattering (DLS) as in Table 10. The uncoated nanostructured lipid carriers had a mean size of 160.3 nm and a relatively wide size distribution (PDI = 0.652) which implies a moderate heterogeneity. Chitosan coating slightly raised the particle size to 172.25 ± 5.09 nm and significantly lowered PDI to 0.072 indicating enhanced uniformity and dispersion stability.
The minimal size growth after coating with chitosan is evidence of the coating of the cationic polymer on the surface of the lipid nanoparticle. This monolayer of chitosan not only increased the hydrodynamic diameter but also provided a stability increase of the particles due to steric and electrostatic stabilization. The PDI decreased significantly, indicating that it is passed to a more monodisperse system, in accordance with previous findings of chitosan-coated lipid nanoparticles, which highlight the repulsive effect of surface charges of the polymer in preventing aggregation.

Table 7. Comparison of Particle Size and PDI for Uncoated and Chitosan-Coated NLCs

Formulation	Particle Size (nm)	PDI
Uncoated NLC	160.3 ± 4.1	0.652 ± 0.015
CH-NLC	172.25 ± 5.09	0.072 ± 0.008

The fact that the homogeneity of the particles has been improved after chitosan coating, is an indicator of high compatibility between chitosan and the lipid matrix in Figure 4. This coating procedure minimized the energy difference among the particles by stabilizing interfacial tension and therefore coalescence was minimized. A PDI less than 0.1 implies a near-monolithic size distribution that is applicable to consistent behaviour of drug delivery systems. Moreover, a size range of about 170 nm is thought to be optimal when delivered orally, the range strikes a balance between increased dissolution and intestinal uptake.

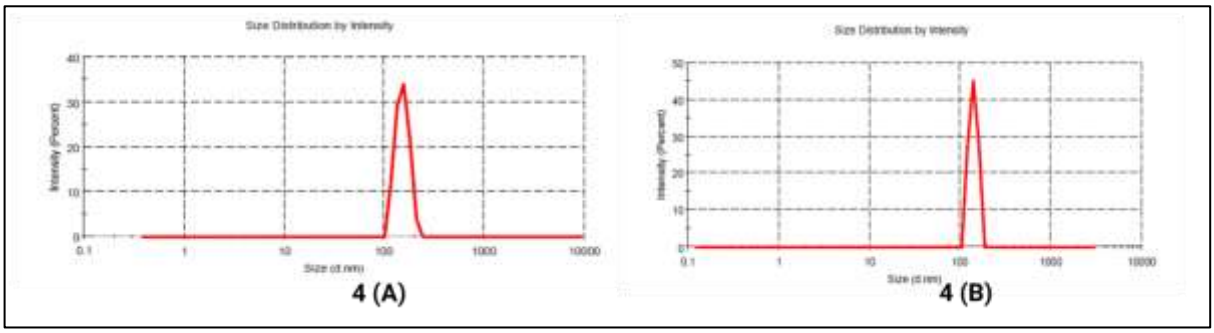

Fig. 4: Particle size distribution of Azilsartan medoxomil-loaded NLCs. (A) Uncoated NLCs (B) Chitosan-coated NLCs (CH–NLCs).

Zeta Potential (ζ-potential)
The ζ-potential of particles and observed a clear difference in surface charge before and after chitosan coating. Uncoated NLCs displayed a potential of −37.0 mV ± 9.24 mV, probably due to ionized fatty acids and surfactant residues in the nanoparticle interface. As shown in Table 8, after chitosan coat the ζ-potential changed and a charge of +36.2 mV ± 4.84 mV was reached confirming that electrostatic adsorption of the cationic polymer into the anionic lipid phase.
Reversal of this charge not only confirms proper coating but also provides greater colloidal stability, enhancing electrostatic repulsion between particles, minimizing aggregation and improving redispersibility upon storage. The

beneficial positive charge imparted by the amine functional group is expected to enhance mucoadhesive potential upon oral administration, leading to interactions with negatively charged mucosal membranes and potentially prolonging residence time or absorption in the GI tract (Fig. 5).

Table 8. ζ-potential Values of NLCs Before and After Chitosan Coating

Formulation	Zeta Potential (mV)	Interpretation
Uncoated NLC	- 37.0 ± 9.24	Stable negative charge; uncoated surface
Chitosan Coated NLC (CH-NLC)	+ 36.2 ± 4.84	Charge reversal confirms chitosan adsorption; enhanced colloidal stability

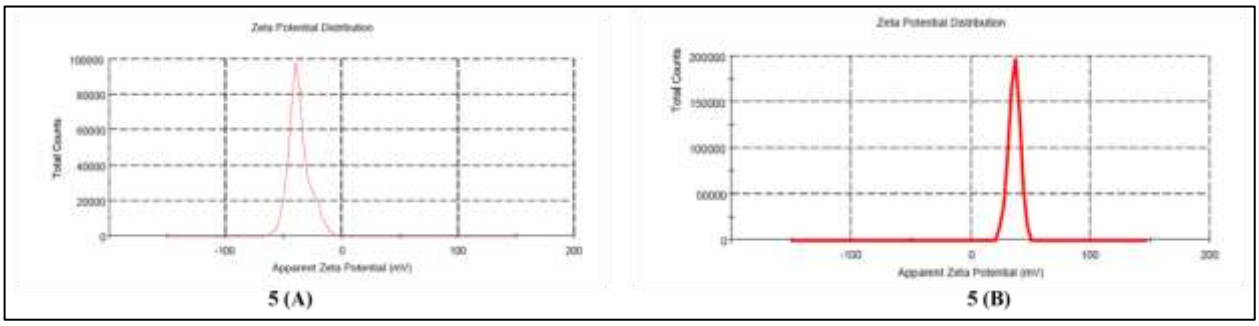

Fig. 5: Zeta potential distribution of Azilsartan medoxomil formulations. (A) Uncoated NLCs showing negative surface charge. (B) Chitosan-coated NLCs showing positive surface charge reversal after coating.

An electrostatic interaction between protonated chitosan and the negatively charged lipid interface is corroborated by the change in ζ-potential from negative to positive. The high ζ-potential (+36.2 mV) suggests strong repulsive forces, ensuring good colloidal stability.

The values of particle size, PDI, and ζ-potential confirms that AZM-loaded CH-NLCs were successfully formulated with small particle size, high monodispersity, and a positive surface charge, ensuring nanocarrier stability in the gastrointestinal (GI) environment, while supporting controlled release and improved mucoadhesive behaviour.

Entrapment Efficiency (EE%)

Result indicates a significant enhancement in entrapment efficiency from 65.23% (NLC) to 85.04% (CH-NLC) as shown in table 9. This enhancement is indebted to the polystyrene microscopic layer formed by chitosan coating, which inhibits drug leakage & diffusion throughout the processing. Hydrogen bonding and electrostatic interactions lead to compactness of the matrix, as well as drug occlusion.

The higher EE in this case correlates with lower PDI and positive ζ-potential, reducing the chances of drug loss and proving improved structural stability which further bolsters overall formulation efficiency (Figure 6).

Table 9. Entrapment Efficiency of Uncoated and Chitosan-Coated AZM-Loaded NLCs

Formulation	Entrapment Efficiency (% ± SD)	Interpretation
Uncoated NLC	65.23 ± 2.15	Moderate encapsulation; partial drug leakage
CH-NLC	85.04 ± 2.61	Enhanced encapsulation due to chitosan polymer barrier

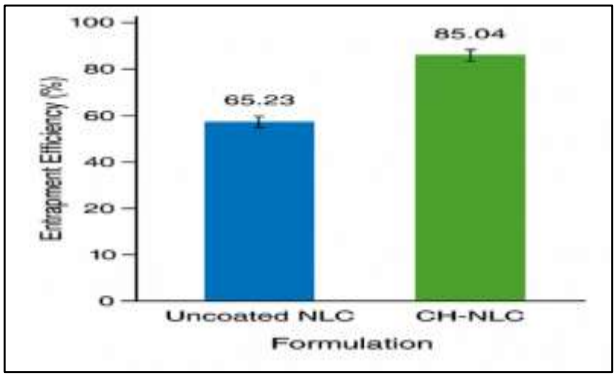

Fig. 6: Entrapment efficiency comparison between uncoated and chitosan-coated NLCs of Azilsartan medoxomil. Error bars represent mean ± SD (n = 3)

Physicochemical analyses indicated improved stability, uniformity, drug encapsulation, and partial amorphization of AZM following chitosan coating, supporting enhanced solubility and sustained release.

SEM Analysis

SEM analysis was indicative of formation of lipid nanospheres, suggested that uncoated NLCs were spherical in shape with smooth surfaces. The surface of CH-NLCs was slightly rougher, which can be explained by chitosan deposition (Figure 7), while they maintained their spherical shape.

The morphological difference serves as evidence of surface modification and uniform coating, while the lack of aggregation shows good colloidal stability. The results are also in agreement with DLS determined particle-size measurements, which indicated a slight increase in particle size without loss of homogeneity.

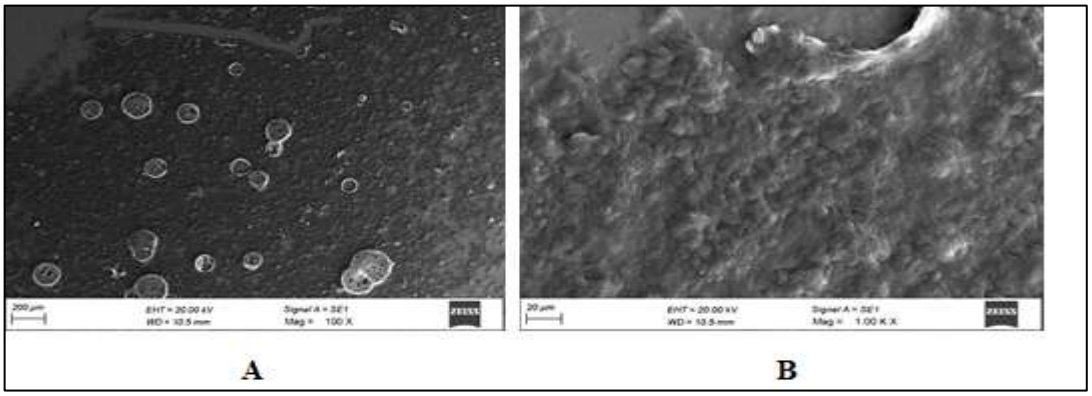

Fig. 7: SEM images of Azilsartan medoxomil-incorporated formulations. (A) Uncoated NLCs displaying smooth spherical morphology.
(B) Chitosan-coated NLCs showing discrete spherical particle showing good stability without aggregation, shows slight roughened surface indicative of coating.

FTIR Analysis

AZM showed characteristic peaks at 1706 cm^{-1} (C=O), 1624 cm^{-1} (C=N), and 1264 cm^{-1} (C–O–C), confirming its chemical integrity. In NLCs, reduced intensity and peak overlap (≈1650 cm^{-1}) indicated hydrogen bonding between AZM and the lipid matrix. In CH-NLCs, these peaks shifted or disappeared, with new broad bands at ~3450 cm^{-1} (O–H/N–H) and ~1550 cm^{-1} (amide II), confirming electrostatic interactions and successful encapsulation (Figure 8).

Overall, these spectral changes demonstrate molecular compatibility and incorporation of AZM without chemical degradation.

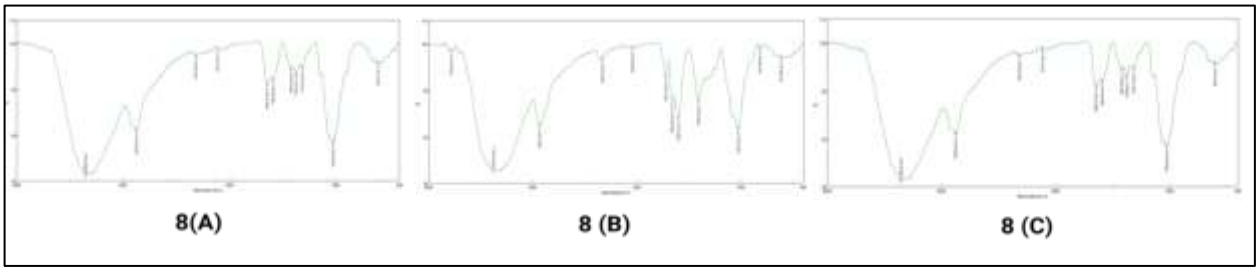

Fig. 8: FTIR spectra of formulation components. (A) Azilsartan medoxomil. (B) NLC (C) Coated NLCs formulation.

XRD Analysis

XRD is widely applied for substrates in crystalline state characterization, here it was used to evaluate crystalline state of AZM during encapsulation process. Pure AZM showed prominent peaks (5°–35° 2θ), confirming its crystalline. Decreased intensity and peak broadening in the NLCs indicated partial amorphization of drug and embedding it within the lipid matrix. The CH-NLCs showed a wider diffuse halo without distinct peaks, consistent with a completely amorphous drug and fully molecularly dispersed in the lipid–polymer network (Figure 9).

These characterization studies demonstrate that chitosan coating significantly improved formulation stability, encapsulation and structure conversion of AZM in the nanostructured lipid matrix. The significant enhancement of entrapment efficiency (EE) and transformation of morphology solid from crystalline to amorphous suggests the strong intermolecular interactions between AZM, chitosan as well as lipid core.

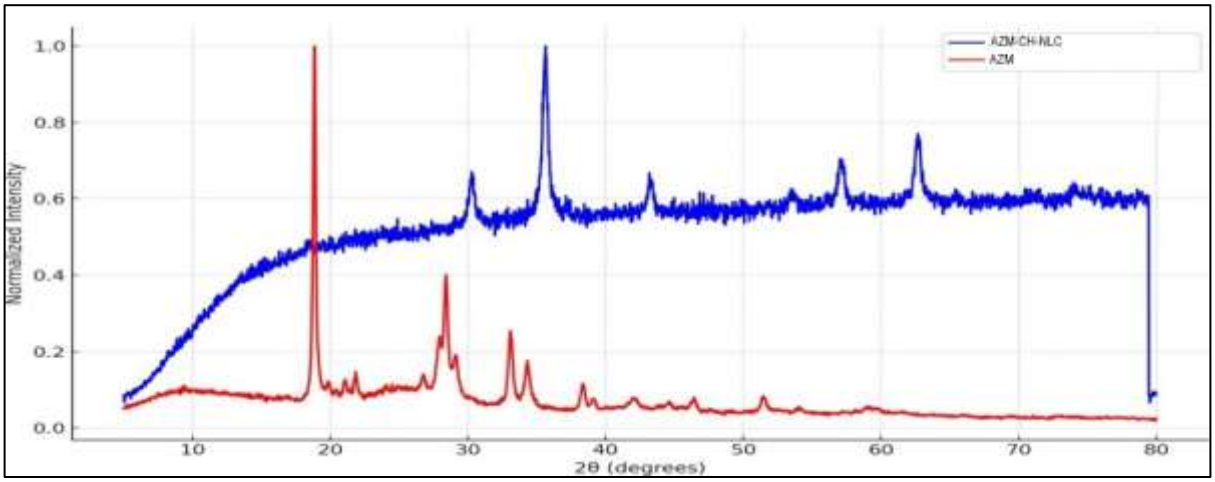

Fig. 9: X-ray Diffraction of Azilsartan medoxomil and its formulations

DSC

AZM showed a sharp endothermic peak at 232.9 °C (ΔH = 22 J/g), which is typical for its crystalline nature and high lattice energy. This unique melting transformation corresponds to the drug self-crystallization and low water solubility. For instance, the uncoated NLC formulation showed a wide endothermic transition at approximately 84 °C (ΔH = 12.98 J/g) which corresponded to the melting of the Compritol–oleic acid lipid matrix. The significant reduction in peak intensity and enthalpy suggests partial solubilisation of AZM within the lipid matrix and a decrease in overall crystallinity, indicating the successful entrapment of the drug in a less ordered lipid environment.

The chitosan-coated NLC (CH-NLC) presented the same melting transition at 84.26 °C (ΔH = 82.63 J/g), but with a modified thermal profile in comparison to uncoated NLCs. The higher enthalpy and loss of the drug crystalline endotherm validations the more stable amorphous dispersion formation joint with stronger polymer–lipid–drug interaction. The results further reveal that the chitosan coating did not alter the structural characteristics of lipid matrices but improved molecular dispersion of AZM within the matrix due to hydrogen bonding and electrostatic interactions.

The DSC data corroborate the findings of XRD and FTIR analyses, confirming amorphization of AZM and establishment of molecular-level compatibility between the drug, lipid, and chitosan. This amorphous transformation is will contribute to enhanced solubility, dissolution rate, and stability of the CH-NLC formulation.

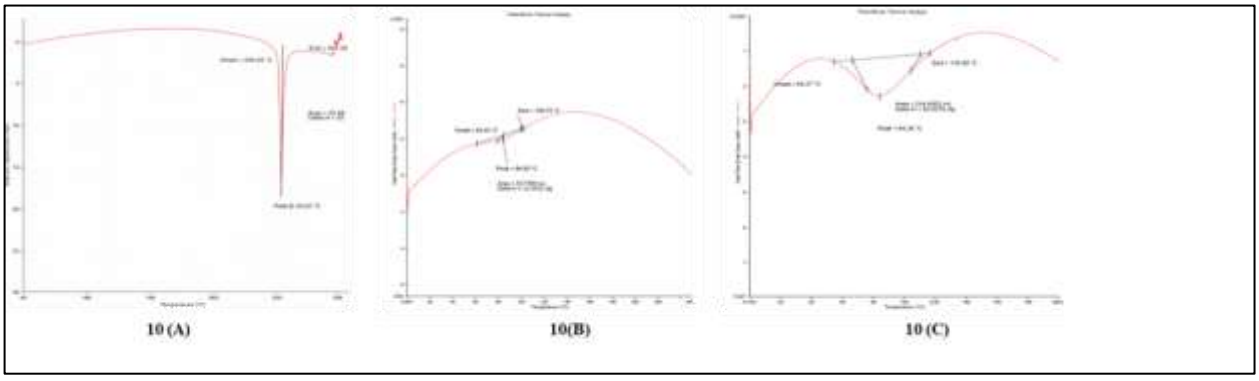

Fig. 10: DSC thermograms of Azilsartan medoxomil and its formulations. (A) Pure drug. (B) AZM-NLC. (C) CH- NLC

The DSC results confirm that AZM is molecularly dispersed in both NLC and CH-NLC matrices, leading to the disappearance of its characteristic crystalline endotherm. Such amorphization enhances apparent solubility and dissolution, supporting the sustained release observed in kinetic studies.

In Vitro Drug Release

The results indicated a marked difference in the rate and extent of AZM release over 24 hours among uncoated and chitosan-coated NLCs. As expected, the release profile for the uncoated system revealed an early burst in release within hour 1 and thereafter by a descending trend over time. This early release is in line with the relative DNA concentration near to particle outer layer or being loosely kept within lipid matrix of AZM.

Chitosan-coated NLCs displayed a relatively more controlled release profile. In the early phase, release was much slower and uniform, showing evidence for the polymer layer as a diffusional barrier. Cumulative release from the coated system at 24 h was about -92%, exceeding released from uncoated NLCs. This shows that chitosan coating did not limit the total extent of release, but rather it played a role in the progression.

The coated formulation produced a controlled release pattern that supports sustained exposure. For a drug such as AZM, which has poor solubility and benefits from prolonged absorption windows, this type of profile is advantageous.

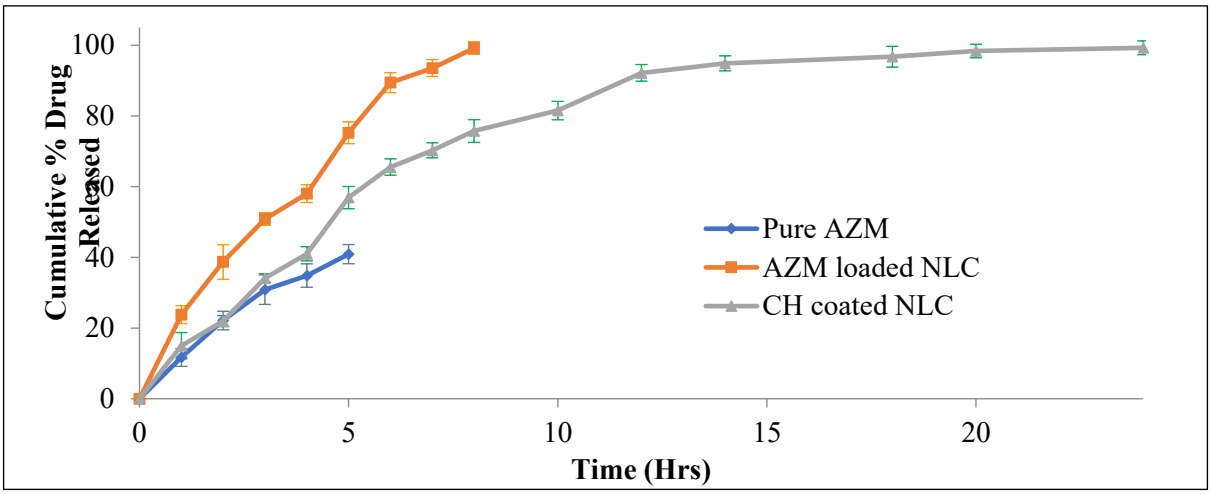

Fig. 11: In vitro drug release of pure AZM, AZM loaded NLC and CH coated NLC at phosphate buffer pH 6.8 maintained at 37 ± 0.5 °C

Release Kinetics

The coated and uncoated NLCs followed the Higuchi model with the correlation coefficients > 0.97, suggesting that these are the best fit models of drug release from both systems. The observations indicate that release was mainly controlled via diffusion through the lipid matrix.

Values of the model exponent (n) obtained from the Korsmeyer–Peppas model were in the range for anomalous transport, suggesting that despite being diffusion dominated, swelling or relaxation of lipid–polymer interface assisted medication release. Using the Hixson–Crowell model, lower values were associated with poor correlations which suggested that the change in geometry of particles did not like affect the process. These phase encapsulated NLCs exhibited significantly improved alignment with diffusion-based models than the uncoated system. Not surprisingly since a chitosan layer becomes yet another AZM diffusion barrier. The observed kinetic behaviours further validates that a controlled-release character was imparted to the coating without compromising release efficiency.

Table 10. Release Kinetic Model Fitting for AZM NLCs

Formulation	**Best-fit model**	Zero order	First order	Higuchi	Korsmeyer–Peppas	Hixon-Crowel
Chitosan-coated AZM NLC	**R² value**	0.7841	0.992	0.979	0.9339	0.9681

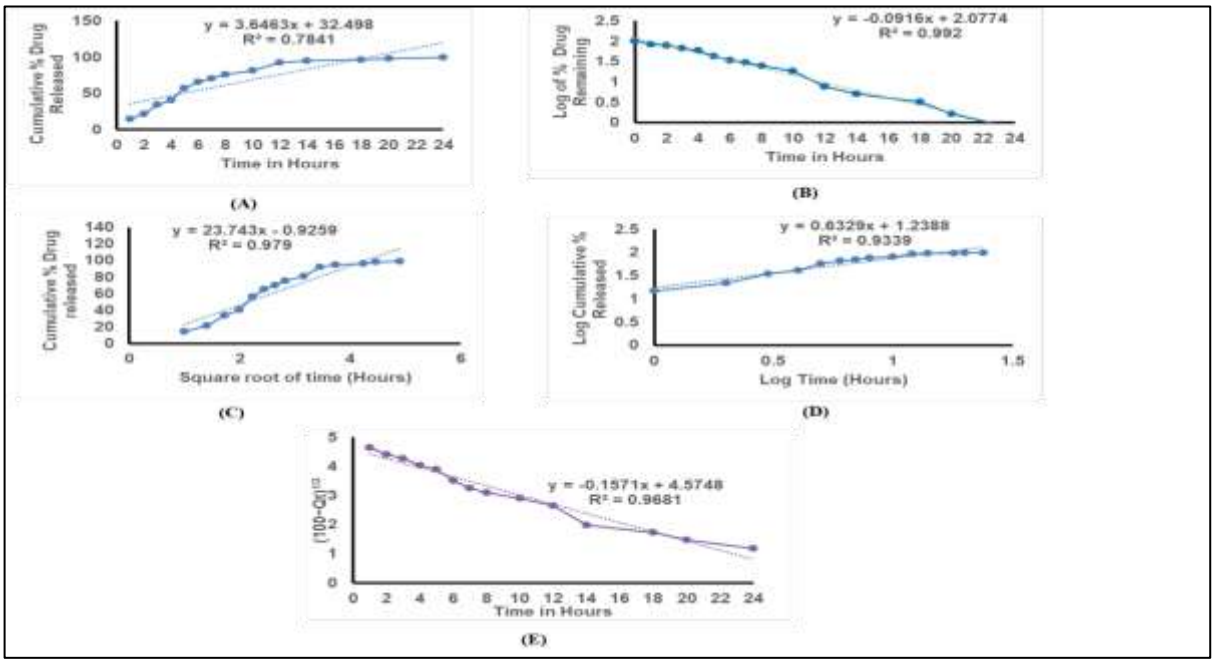

Figure 12. Release kinetics of optimized formulation were fitted to zero-order, first-order, Higuchi, Korsmeyer–Peppas, and Hixson–Crowell models

DISCUSSION

The study aimed to successfully design and optimize chitosan coated AZM incorporated NLCs utilizing QbD approach. The optimized preparation displayed a nanoscale size (172 nm), narrow size distribution, high entrapment efficiency (~85%), and sustained drug release, while BBD Design successfully identified the key parameters governing nanoparticle performance.

The particle size 172 nm falls into the optimal lipid-based oral delivery systems range (150–250 nm for maximally effective colloidal stability). The low PDI confirms the uniform nanoparticles distribution due to efficient homogenization and sonication. A high positive zeta potential confirmed efficient electrostatic interaction between the negatively charged lipid core and protonated chitosan amino groups, which improved dispersion stability and inhibited aggregation.

High entrapment efficiency due to imperfect lipid matrix of nanostructured lipid carriers that creates structural defects enhancing drug accommodation in comparison with highly crystalline solid lipid systems. An additional entrapment efficiency was achieved by introducing a polymeric shell due to the chitosan coating, who impedes drug diffusion and enhances structural stability (electrostatic stabilization).

A continuous drug release over 24 h followed the Higuchi/Korsmeyer Peppas model (diffusion-controlled kinetics) which is attributed to: (i) entrapment of AZM inside the solid–liquid lipid matrix forming a barrier, (ii) slow diffusion of AZM released from the lipid core and (iii) regulating diffusion. The solid state characterization of AZM showed its conversion into amorphous or molecularly-dispersed forms, which correlated with improved dissolution and formulation performance. Nanjundasamy et al. Drug development in ABAP polymer solution method: An example of QbD methodology for sustainable pharmaceutical education and research. This reduced the need for empirical trial-and-error experimentation.

Limitations: No in vivo pharmacokinetic testing was conducted, and despite the positive surface charge suggesting potential mucoadhesion, direct mucoadhesion experiments were not performed.

Future Studies: To establish translational potential, ex vivo intestinal permeation, in vivo pharmacodynamic/pharmacokinetic studies, long-term stability assessment under ICH conditions and feasibility for scale-up need to be addressed. CH-NLCs provide a systematically optimized delivery platform for poorly soluble AZM with nanoscale physicochemical properties, high loading and sustained release. Designing excellent formulation is the first step, but QbD principles setup a good groundwork for implementing future, more efficient formulation development.

CONCLUSION

QbD approach was used for designing and optimization of Azilsartan medoxomil loaded chitosan-coated nanostructured lipid carriers (CH-NLCs). This optimized formulation was able to obtain nanoscale particles (172 nm), significant drug loading (~85%) and sustained release for 24 hours. The zeta potential and colloidal stability were improved by chitosan coating. Drug encapsulation in the solid-state was confirmed through characterization studies which also ruled out any possibility of chemical incompatibility. The diffusion barriers allowing sustained release were followed by the lipid matrix as well as chitosan coating. However, further studies like mucoadhesion and in vivo pharmacokinetic were still needed.

ACKNOWLEDGEMENTS

The authors extend their gratitude to Karpagam Academy of Higher Education, Coimbatore, Tamil Nadu, India for providing necessary facilities and support for this research.

AUTHOR CONTRIBUTION

Study Conception and Design: JP and SG; Data Collection: JP; Analysis and Interpretation of Results: JP and SG; Draft Manuscript: JP. All authors reviewed the results and approved the final version of the manuscript.

FUNDING

None to Declare.

CONFLICT OF INTEREST (If any)

None to Declare.

ETHICS APPROVAL

None to Declare.

DECLARATION OF GENERATIVE AI AND AI-ASSISTED TECHNOLOGIES IN THE WRITING PROCESS

During the preparation of this work, the author (s) used Quillbot to improve the language, grammer and readability of the manuscript. The author(s) reviewed and edited the output as necessary and accept full responsibility for the content of the final manuscript.

REFERENCES

1. Kumar G, Virmani T, Pathak K, Kamaly O, Saleh A. Central composite design implemented azilsartan medoxomil loaded nanoemulsion to improve its aqueous solubility and intestinal permeability. Pharmaceuticals. 2022; 15(11):1343. doi:10.3390/ph15111343.

2. Scioli-Montoto S, Santander-Ortega MJ, Martín-Banderas L. Novel phenobarbital-loaded nanostructured lipid carriers: QbD optimization and stability evaluation. Front Chem. 2022; 10:908386. doi:10.3389/fchem.2022.908386.
3. Cunha S, Costa CP, Moreira JN, Sousa Lobo JM, Silva AC. Using the Quality by Design (QbD) approach to optimize formulations of lipid nanoparticles and nanoemulsions: a review. Nanomedicine (Lond). 2020; 15(19):1851–1871. doi:10.2217/nnm-2020-0101.
4. Alam T, Pandit J, Vohora D, Aqil M, Ali A, Sultana Y. Quality-by-design based development of nanostructured lipid carriers: a risk-based approach for oral delivery of lamotrigine. Explor Med. 2022; 3:617–638. doi:10.37349/emed.2022.00118.
5. Ponnusamy J, Gopal S. Nanostructured Lipid Carriers: Enhancing Delivery of Poorly Soluble Drugs. Current Nanomaterials. 2026; 11(3): 307-321. doi:10.2/74/0124054615364839250623094350.
6. Gaba B, Khan S, Haider MF, Alam T, Baboota S, Sahu S, et al. Chitosan-coated nanostructured lipid carriers for oral delivery of silymarin: in vitro and in vivo evaluation. J Microencapsul. 2020; 37(5):385–395. doi:10.1080/02652048.2020.1765545
7. Chachanidze R, Xie K, Massaad H, Nguyen H, Schlenoff JB. Structural characterization of interfacial self-assembly of chitosan with oppositely charged surfactants. Langmuir. 2021; 37(40):11897–11909. doi: 10.1021/acs.langmuir.1c02023
8. Ma J, Yang Y, Sun Y, Sun J. Optimization, characterization, and in vitro/in vivo evaluation of azilsartan nanocrystals. Asian J Pharm Sci. 2021; 16(2):344–352. doi: 10.1016/j.ajps.2020.06.004
9. Patel P, Khan S, Desai J, Alqahtani S, Shah V. Nanotechnology-based strategies for extended-release delivery of angiotensin receptor blockers: a comprehensive review. Chimia (Aarau). 2023; 77(9):761–772. doi:10.2533/chimia.2023.761
10. Brown P, Zhao X, Singh M, Williams R, Chen H, et al. Entrapment efficiency of chitosan-based nanocarriers: a formulation approach. J Control Release. 2022; 342:45–58. doi: 10.1016/j.jconrel.2021.12.010
11. Nguyen T, Lopez M, Choi R, Kim S, Lee H. Impact of lipid and surfactant concentrations on drug encapsulation and release properties of nanostructured lipid carriers. J Appl Pharm Sci. 2021; 11(5):75–89. doi:10.7324/JAPS.2021.110509
12. Ghogare NS, Sharma P, Patil SR, Jadhav KR. Nanostructured lipid carriers: an emerging vehicle for drug delivery. Asian J Pharm Clin Res. 2025; 18(2):1–10. doi:10.22159/ajpcr. 2025.v18i2.47425
13. Mall J, Alqahtani S, Ahmad MZ, Ahmad J, Ahmad FJ. Nanostructured lipid carriers as a drug delivery system: recent advances and future perspectives. Int J Pharm Investig. 2024; 14(3):173–182. doi: 10.4103/ijpi.ijpi_121_23
14. Abdelmonem R, Eissa E, Hassan A, Farag AM, Shalaby A. Fabrication and optimization of nanostructured lipid carriers for ocular delivery: a QbD approach. Pharmaceutics. 2022; 14(9):1884. doi:10.3390/pharmaceutics14091884
15. Hidayat AF, Wahab A, Rosidah R, et al. Risk assessment and optimization of lipid nanocarriers using the Quality by Design approach: a systematic review. Pharmaceutics. 2025; 17(2):263. doi:10.3390/pharmaceutics17020263
16. Pyo YC, Tran P, Kim DH, Park JS. Chitosan-coated nanostructured lipid carriers of fenofibrate: formulation and characterization. Colloids Surf B Biointerfaces. 2020; 193:111331. doi: 10.1016/j.colsurfb.2020.111331
17. Khan S, Ullah S, Khan RA, Ali S, Iqbal J, et al. An overview of nanostructured lipid carriers and their applications. Int J Pharm. 2022; 606:120954. doi: 10.1016/j.ijpharm.2022.120954
18. López KL, Martínez A, Ramírez M, Ruiz ME, et al. Solid lipid nanoparticles and nanostructured lipid carriers: production methods and applications. Front Nutr. 2023; 10:10221859. doi:10.3389/fnut.2023.10221859
19. Viegas C, Veiga F, Pires I, Ribeiro AJ, Figueiras A. An insight on lipid nanoparticles for therapeutic proteins. Int J Pharm. 2022; 614:121405. doi: 10.1016/j.ijpharm.2022.121405
20. Haider F, Rahman M, Singh A, Gupta A, Jain N, Mishra V. Surface-engineered chitosan-coated nanostructured lipid carriers for enhanced oral drug delivery. Future J Pharm Sci. 2025; 11:97. doi:10.1186/s43094-025-00738-0
21. Hassan DM, Ibrahim MA, El-Gindy AE, El-Sisi AM, et al. Chitosan-coated nanostructured lipid carriers for effective brain delivery: development and evaluation. Int J Nanomedicine. 2023; 18:3431–3444. doi: 10.2147/IJN.SXXXXXX
22. Elmowafy M, Abdel-Mottaleb MM, Shalaby K, Abd-Alrassol M, Eissa M, El-Aassar MR, et al. Chitosan-coated nanostructured lipid carriers for brain delivery of rivastigmine. J Drug Deliv Sci Technol. 2021; 63:102375. doi: 10.1016/j.jddst.2021.102375
23. Haider F, Parveen R, Baboota S, Ali J, Ahmad FJ. Surface-engineered chitosan-coated nanostructured lipid carriers for intranasal delivery of oxcarbazepine. Future J Pharm Sci. 2025; 11:155. doi:10.1186/s43094-025-00855-x
24. Jain A, Jain SK. Chitosan-coated nanostructured lipid carriers for targeted delivery of paclitaxel to breast cancer cells. Int J Nanomedicine. 2020; 15:4767–4781. doi:10.2147/IJN.S252467
25. Pereira RR, Santos F, Foggi MV, Almeida MC, Campos JM, et al. Development and optimization using Box–Behnken design: application to lipid nanocarriers. Pharmaceutics. 2020; 11(6):284. doi:10.3390/pharmaceutics11060284
26. Sangeetha S, Kumar V, Rajan R, Murugan N, Iyer SS. Formulation design, optimization, and evaluation of solid lipid nanoparticles via Box–Behnken design. J Adv Pharm Technol Res. 2024; 15(1):45–55. doi: 10.4103/japtr.japtr_102_23
27. Gilani SJ, Maqbool I, Hussain T, Khan I, Rehman A. Chitosan-coated luteolin nanostructured lipid carriers: optimization and evaluation. Coatings. 2021; 11(2):158. doi:10.3390/coatings11020158
28. Unnisa A, Yugandhar P, Sreeharsha N, Reddy KJ, Al-Dhubiab BE, et al. Development of dapagliflozin solid lipid nanoparticles using Box–Behnken design: physicochemical characterization. Pharmaceuticals. 2022; 15(5):568. doi:10.3390/ph15050568
29. Abo El-Enin HA, Elkomy MH, Naguib IA, Ahmed MF, Alsaidan OA, Alsalahat I. Lipid nanocarriers overlaid with chitosan for brain delivery of berberine via the nasal route. Pharmaceuticals. 2022; 15(3):281. doi:10.3390/ph15030281

30. Buya AB, Yame T, Nambita B, Mutwala A, Chitanda JM, et al. From lab to industrial development of lipid nanocarriers: challenges and QbD applications. Adv Drug Deliv Rev. 2024; 210:114510. doi: 10.1016/j.addr.2024.114510
31. Severino P, da Silva CF, Andrade F, de Souza MC, Santana MHA, Souto EB. Surface modification of nanostructured lipid carriers with chitosan for the delivery of curcumin. Int J Biol Macromol. 2020; 150:855–863. doi: 10.1016/j.ijbiomac.2020.01.241
32. Khan B, Ahmad J, Rahman M, Alam T, Ahmad MZ, et al. Box–Behnken design-assisted optimization in pharmaceutical systems: an overview. J Control Release. 2025; 380:25–41. doi: 10.1016/j.jconrel.2024.12.015
33. Pyo YC, Tran P, Kim DH, Park JS. Chitosan-coated nanostructured lipid carriers of fenofibrate with enhanced oral bioavailability and efficacy. Int J Pharm. 2020; 583:119404. doi: 10.1016/j.ijpharm.2020.119404
34. Abdellatif MM, Shohdy JN, El-Setouhy DA, Hamed MIA, Rofaeil BF, et al. Chitosan-decorated nanostructured lipid carriers for augmented oral bioavailability of velpatasvir: D-optimal optimization, in silico, in vitro, ex vivo and in vivo studies. Int J Biol Macromol. 2023; 234:123107. doi: 10.1016/j.ijbiomac.2023.123107